Frontiers in Bioscience Landmark

Front. Biosci. (Landmark Ed) **2025**; 30(7): 26076
https://doi.org/10.31083/FBL26076

Original Research

The Role of THBS4 in Chronic Kidney Disease Fibrosis: From Clinical Observations to Molecular Mechanisms

Xu Yan[1], Kun Zhao[2], Ye Yao[1], Lihui Wang[1], Wei Shan[3], Yan Zhang[1,*]

[1]Department of Nephrology, The Second Affiliated Hospital of Qiqihar Medical University, 161006 Qiqihar, Heilongjiang, China
[2]College of Basic Medical Sciences, Qiqihar Medical University, 161006 Qiqihar, Heilongjiang, China
[3]Department of Laboratory Medicine, The Second Affiliated Hospital of Qiqihar Medical University, 161006 Qiqihar, Heilongjiang, China
*Correspondence: Zhy286303443@qmu.edu.cn (Yan Zhang)

Academic Editors: Vesna Jacevic and Esteban C. Gabazza
Submitted: 9 August 2024 Revised: 29 October 2024 Accepted: 29 November 2024 Published: 29 July 2025

Abstract

Background: Chronic kidney disease (CKD), driven by progressive renal fibrosis, lacks effective therapeutic targets. This study investigates thrombospondin-4 (THBS4) as a novel mediator of CKD-related fibrosis and explores its mechanistic basis. **Methods**: This study collected 100 patients diagnosed with chronic kidney disease and 30 healthy individuals. Enzyme-linked immunosorbent assay (ELISA) analysis was conducted to assess the expression of THBS4 in CKD patients. Mouse unilateral ureteral obstruction (UUO) renal fibrosis model and Human Kidney-2 (HK2) cell fibrosis model were constructed to analyze the expression changes of THBS4 in renal fibrosis. To examine the effects of inhibiting THBS4 expression on the process of renal fibrosis, these two models were analyzed using Sirius red staining, Masson staining, immunohistochemistry, real-time quantitative PCR (qPCR) and western blot methods. **Results**: The expression of THBS4 in the serum of CKD patients was found to be significantly higher ($p < 0.05$), and its concentration showed a negative correlation with the eGFR levels ($r = –0.77$, $p < 0.05$) and an increase corresponding to the progression of CKD stages ($p < 0.05$). THBS4 expression was dramatically increased in UUO-treated mouse kidneys as well as in TGF-β1-stimulated HK2 cells ($p < 0.05$). *In vitro*, the expression of renal fibrosis-associated proteins was also significantly reduced after interfering with THBS4 expression ($p < 0.05$). UUO-induced renal fibrosis and related protein expression were suppressed in *THBS4* knockdown mice when compared to control mice ($p < 0.05$). The levels of p-AKT and p-PI3K exhibited a significant rise in conjunction with the onset of renal fibrosis ($p < 0.05$). The expression of p-AKT as well as p-PI3K showed a significant reduction upon inhibition of THBS4 expression ($p < 0.05$). Insulin-like growth factor 1 (IGF-1) treatment reversed these effects. **Conclusion**: THBS4 was significantly overexpressed in CKD patients. By suppressing the expression of proteins associated with renal fibrosis and inhibiting the activation of the PI3K/AKT pathway, THBS4 has the potential to mitigate renal fibrosis.

Keywords: chronic kidney disease; thrombospondin-4; renal fibrosis; fibrosis-associated protein; PI3K/AKT pathway

1. Introduction

Chronic kidney disease (CKD) is a common disease in the global periphery. Epidemiologic studies have shown that the incidence and prevalence of CKD has risen by nearly 90% over the past 30 years [1]. This is expected to increase as the population ages. World Health Organization surveys have shown that the annual mortality rate attributed to CKD is estimated to range from 50 to 100 million deaths. It is estimated that by 2040, CKD will be the fifth leading cause of death worldwide [2]. The lack of disease awareness contributes significantly to the elevated morbidity and mortality rates associated with CKD. Since the early stages of CKD have no clinical symptoms, this stage is easily overlooked and undertreated. It is estimated that about 94% of patients with mild to moderate decline in renal function and about 48% of patients with severe renal insufficiency are undiagnosed [3,4].

Renal fibrosis plays a crucial role in the advancement of CKD and is regarded as the ultimate shared pathological alteration across various kidney diseases. CKD is characterized by persistent inflammation, which initiates the fibrotic process. The recruitment of inflammatory cells, including lymphocytes, granulocytes, and macrophages, is a result of the inflammatory process. These cells then release transforming growth factor β1 (TGF-β1) [5,6]. TGF-β1 is a potent fibrogenic factor that induces fibroblast activation and extracellular matrix protein synthesis, which promotes cellular fibrosis [7,8]. Renal fibrosis not only contributes to the worsening of renal function, but also exhibits a significant correlation with elevated cardiovascular risk and mortality [9]. Therefore, studies on the mechanisms of fibrosis in CKD are crucial.

A secreted extracellular matrix protein, thrombospondin-4 (THBS4) belongs to the thrombospondin family [10]. As a crucial constituent of the extracellular milieu, THBS4 assumes a pivotal function in cellular attachment, movement, growth, and programmed cell death [11,12]. Recent studies have shown that THBS4 plays a role in the process of wound healing and tissue restructuring through its regulation of extracellular matrix

organization, repair, and remodeling [13,14]. In addition, the mechanism of action of THBS4 is gradually being revealed in cardiovascular diseases, tumor biology, and neurodegenerative diseases [15–17].

While THBS4's significance in other biological systems has been extensively investigated, little is known about its function in CKD, specifically with regard to the procession of renal fibrosis. Our assumption was that THBS4 during CKD could potentially regulate the progression of renal fibrosis by influencing the modulation of extracellular matrix and signaling pathways, including the phosphatidylinositol 3-kinase/serine-threonine kinase (PI3K/AKT) pathway. Further, we tested this hypothesis through clinical sample analysis and animal model studies and investigated the potential of THBS4 as a viable target for therapeutic intervention.

2. Materials and Methods

2.1 Sample Sources

One hundred patients diagnosed with CKD from the Second Affiliated Hospital of Qiqihar Medical University and 30 healthy people were collected for inclusion in this study. Patient inclusion exclusion criteria: Patients attending our clinic were identified as having chronic kidney disease after routine urinalysis and renal function tests. Renal transplant recipients and patients with acute kidney injury were excluded. The baseline data of the patients was recorded at the time of diagnosis (**Supplementary Table 1**), and blood samples were collected simultaneously. Based on the guidelines developed by Kidney Disease: Improving Global Outcomes (KDIGO) [3], patients with CKD can be categorized into five stages based on estimated glomerular filtration rate (eGFR): CKD1 (eGFR, >90 mL/min), CKD2 (eGFR, 60–89 mL/min), CKD3 (eGFR, 30–59 mL/min), CKD4 (eGFR, 15–29 mL/min), and CKD5 (eGFR, <15 mL/min); Where eGFR <60 mL/min/1.73 m^2 indicates abnormal renal function and possible chronic kidney disease. Based on the eGFR values in the patients' baseline data, CKD patients can be categorized into two groups, CKD 1-2 and CKD 3-5, for subsequent studies. The study was approved by the Second Affiliated Hospital of Qiqihar Medical University Ethics Committee (ethics number: [2022]0815-8-2) and subjects participating in the study gave informed consent. This study strictly adheres to the ethical principles and guidelines of the Declaration of Helsinki.

The study procured male C57BL/6 mice, aged 6–8 weeks, with an average weight of 25–30 grams, and *THBS4*-knockdown mice (shRNA-*THBS4*) were generated by intravenous injection of AAV9 particles expressing shRNA targeting *THBS4* (Guangzhou Ruige Bio-Tech Co., Ltd., Guangzhou, China), while control mice (scramble) received AAV9-scramble-shRNA (Guangzhou Ruige Bio-Tech Co., Ltd., Guangzhou, China). A total of 12 mice were used in this study. All animal experiments comply with the international ethical standards for experimental animals and the regulations designated by the Second Affiliated Hospital of Qiqihar Medical University Ethics Committee (ethics number: [2022]0815-8-2). Human-derived renal tubular proximal epithelial cell line HK2 was purchased from Hunan Fenghui Biotechnology Co., Ltd. (CL0144, Changsha, Hunan, China).

2.2 Unilateral Ureteral Obstruction (UUO) Model

Six 6–8 week-old healthy mice were prepared for each group. The mice were anesthetized by intraperitoneal injection of 2% sodium pentobarbital (4 mL/kg). In the experimental group, an incision was made on the dorsal side of the mice to reveal the left ureter. The ureter was then tied off using two 4.0-gauge silk sutures (0.35 mm diameter). The sham-operated group was operated only without ureteral ligation. 14 days later, mice were anesthetized as described above and then cervical dislocation was performed on the mice and kidney tissues were collected. Some kidneys were fixed with 4% formalin, followed by dehydration and paraffin embedding, and the remaining tissues were stored in a cryogenic liquid nitrogen environment for preservation [18].

2.3 Cell Culture and Processing

HK2 cells were cultured in Dulbecco's Modified Eagle Medium/Nutrient Mixture F-12 (DMEM/F12; C11330500BT, Gibco, Grand Island, NY, USA) supplemented with 10% fetal bovine serum (FBS; 10270106, Gibco, Grand Island, NY, USA) and 1% penicillin/streptomycin (15140122, Gibco, Grand Island, NY, USA) at 37 °C under 5% CO_2. For experimental interventions, cells were divided into six groups: Control (untreated), si-NC (transfected with scramble siRNA), si-*THBS4* (transfected with *THBS4*-specific siRNA; sequence: 5′-CGCCCUGAAUGAUCUCUAUTT-3′; L31520, Beyotime, Shanghai, China), si-NC + TGF-β1 (scramble siRNA + 10 ng/mL TGF-β1; 100-21, PeproTech, Cranbury, NJ, USA), si-*THBS4* + TGF-β1 (*THBS4* siRNA + TGF-β1), and Rescue (*THBS4* siRNA + TGF-β1 + 100 ng/mL IGF-1; HY-P7018, MedChemExpress, Shanghai, China). Transfection was performed using Lipofectamine 3000 (L3000015, Invitrogen, Carlsbad, CA, USA) with 50 nM siRNA at 60% cell confluence. After 6 hours, the medium was replaced, followed by TGF-β1 treatment for 48 hours or insulin-like growth factor 1 (IGF-1) treatment for 24 hours as indicated. The short tandem repeat (STR) validation and *Mycoplasma* detection results for all cell lines were confirmed. The mycoplasma test results were negative.

2.4 Immunohistochemical Assay

Sections were routinely deparaffinized and heat repaired in antigen repair solution for 35 min, and then im-

munohistochemical (IHC) assays were performed according to the instructions of IHC kit (36311ES50, Yeasen Biotechnology, Shanghai, China). The sections were treated with 3% H_2O_2 at a temperature of 4 °C for a duration of 10 minutes, followed by rinsing with phosphate balanced solution (PBS) for three cycles, each lasting 2 minutes; incubated with Avidin at room temperature for 15 min and rinsed with PBS for three cycles, each lasting 2 minutes/3 times; exposed to Biotin for a duration of 15 minutes at ambient temperature, followed by a 5-minute rinse with PBS; subsequently, the blocking solution was introduced and the sections were subjected to a 20-minute blocking process at ambient temperature. The blocking solution was removed, and the sections were exposed to the primary antibody (THBS4, 1:100, CSB-PA562708, Wuhan Huamei BIOTECH, Wuhan, China). for an extended period at a low temperature of 4 °C. Wash with PBS for a duration of 5 minutes, followed by incubation with the secondary antibody (Horseradish Peroxidase (HRP) Goat Anti-Rabbit, 1:2000, ab205718, abcam, Cambridge, UK) at ambient temperature for a period of 30 minutes. Rinse with PBS for 5 min, add 3-3′-diaminobenzidine (DAB) chromogenic solution for 5–10 min, rinse with water, re-stain, dehydrate, clear and seal. For the quantitative analysis of immunohistochemical staining, the intensity of staining was evaluated using the H-score method.

2.5 Periodic Acid-Schiff Stain (PAS), Masson and Picro Sirius Red (PSR) Staining

Paraffin sections were deparaffinized and subjected to PAS staining as described below. The sections were subjected to a 15-minute immersion in a 1% solution of periodic acid, followed by rinsing with water for 2–3 cycles. The sections underwent staining by being immersed in Schiff's solution for a duration of 10–30 minutes, followed by rinsing with water 2–3 times. Stained with Haematoxylin for 1–2 min, washed 2–3 times in water. Immersion in 1% hydrochloric acid-ethanol for 5 sec, wash in water 2–3 times. Ammonia counterblue for 5–10 sec, rinsed in water, dehydrated, transparent, and sealed. Masson (ALP87019, Thermo Fisher Scientific, Waltham, MA, USA) and Picro Sirius Red (PSR) (36324ES60, Yeason Biotechnology, Shanghai, China) staining was performed according to the operating instructions of the kit. Staining results were quantitatively analyzed using Image-Pro Plus software (5.0.2, Media Cybernetics, Rockville Pike, MD, USA).

2.6 Enzyme-Linked Immunosorbent Assay (ELISA)

Patient serum was obtained by collecting patient whole blood and centrifuging the supernatant. The amount of THBS4 was detected based on the instructions of the ELISA kit (XG-E990828, Shanghai Sig Biotechnology Co., Ltd., Shanghai, China). The absorbance value of the test wells at 450 nm was read by an enzyme meter. The formula for calculating the concentration (C) of THBS4 in the samples based on the OD value (OD_sample) is as follows:

$$C = e^{\left(\frac{\left(OD_{sample} - OD_{blank}\right) \times \left(\log_{10}(C_{max}) - \log_{10}(C_{min})\right)}{\left(OD_{max} - OD_{min}\right)} + \log_{10}(C_{min})\right)}$$

Where:

C is the concentration of THBS4 in the sample,

OD_{sample} is the optical density of the sample,

OD_{blank} is the optical density of the blank (background),

C_{max} and C_{min} are the maximum and minimum concentrations of the standard curve, respectively,

OD_{max} and OD_{min} are the corresponding optical densities of the standard curve.

Table 1. qPCR primer sequences (Human).

Genes	Sequence (5′-3′)
COL1A1	Forwards: GATTCCCTGGACCTAAAGGTGC
	Reverse: AGCCTCTCCATCTTTGCCAGCA
FN1	Forwards: ACAACACCGAGGTGACTGAGAC
(encoding Fibronectin)	Reverse: GGACACAACGATGCTTCCTGAG
ACTA2	Forwards: CTATGCCTCTGGACGCACAACT
(encoding α-SMA)	Reverse: CAGATCCAGACGCATGATGGCA
THBS4	Forwards: CCTTCTGAGACAGCAGGTTAAG
	Reverse: GTCGGAGACTGAAACTTGAGAG
GAPDH	Forwards: GGAGCGAGATCCCTCCAAAAT
	Reverse: GGCTGTTGTCATACTTCTCATGG

qPCR, real-time quantitative PCR; COL1A1, collagen type I alpha 1; FN1, fibronectin 1; ACTA2, actin alpha 2; THBS4, thrombospondin-4; GAPDH, glyceraldehyde-3-phosphate dehydrogenase.

2.7 Real-Time Quantitative PCR (qPCR)

Total RNA was extracted from tissues and cells using Trizol reagent (15596018, Invitrogen, Carlsbad, CA, USA). First strand DNA was synthesized by cDNA reverse transcription kit using RNA as a template. The reaction solution was prepared by SYBR Select Master Mix kit (4472919, ABI, Foster City, CA, USA) using DNA as a template. The reaction solution was used to complete quantitative fluorescence assay in a quantitative PCR instrument (Bio-Rad, Hercules, CA, USA) to accomplish quantitative fluorescence detection. The assay results were calculated using the $2^{-\Delta\Delta Ct}$ method. The amplification primer sequences of genes are shown in Table 1 (Human) and Table 2 (mouse).

2.8 Western Blotting (WB)

The Radio Immunoprecipitation Assay (RIPA) lysis buffer was utilized to extract the entire cellular proteins, while the protein concentration was determined using the Bromocresol Green with Albumin (BCA) kit (A55864, Thermo Fisher Scientific, Waltham, MA, USA). The separation of proteins was achieved through the utilization of

Table 2. qPCR primer sequences (mouse).

Genes	Sequence (5′-3′)
Col1a1	Forwards: CGATGGATTCCCGTTCGAGT
	Reverse: TTCGATGACTGTCTTGCCCC
Fn1	Forwards: CGAGGTGACAGAGACCACAA
(encoding Fibronectin)	Reverse: CTGGAGTCAAGCCAGACACA
Acta2	Forwards: GAGGCACCACTGAACCCTAA
(encoding α-SMA)	Reverse: CATCTCCAGAGTCCAGCACA
Thbs4	Forwards: GACGGCTATGTCTGTGGAAAGG
	Reverse: TCCGATGCCATCTCTGTCTGCA
Gapdh	Forwards: GTGCTGAGTATGTCGTGGAG
	Reverse: TCGTGGTTCACACCCATCAC

SDS-PAGE gel electrophoresis. The gel that underwent electrophoresis was transferred onto a polyvinylidene fluoride (PVDF) mold and sealed with 5% skimmed milk for 1 hour at ambient temperature. The gel was subsequently subjected to overnight incubation at a temperature of 4 °C with the primary antibody GAPDH (5174S; 1:1000), collagen type I alpha 1 (COL1A1, 72026; 1:1000), Fibronectin (26836; 1:1000), α-SMA (19245; 1:1000), PI3K (4257; 1:1000), AKT (4691; 1:1000), p-PI3K (4292; 1:1000) and p-AKT (4060; 1:1000) (Cell Signaling Technology, Danvers, MA, USA) and THBS4 (ZY65162R, Shanghai Zeye Biotechnology Co., Ltd., Shanghai, China). After the membrane was washed, it underwent incubation with a secondary antibody (7074; 1:1000, Cell Signaling Technology, Danvers, MA, USA) for 1 hour at room temperature. Developed and photographed. The grayscale values of the protein bands were calculated employing Image 5.0 software (5.0.2, Media Cybernetics, Rockville Pike, MD, USA).

2.9 Statistical Analysis

The statistical analysis of the experimental data was conducted utilizing IBM SPSS statistics 26 software (IBM Corp., Armont, NY, USA). Continuous variables are presented as mean ± standard deviation (SD) or median with interquartile range (IQR) depending on their distribution. The drawing tool is GraphPad Prism8 software (GraphPad, La Jolla, CA, USA). Data that were tested to be normally distributed and significant differences between two groups of data were analyzed by Student's *t*-test. Significant differences between more than two groups of data were analyzed by one-way analysis of variance (ANOVA). Those that were tested not to follow normal distribution were analyzed for significant differences using Mann-Whitney U's nonparametric test. $p < 0.05$ represents significant differences ($*p < 0.05$, $**p < 0.01$, $***p < 0.001$, $****p < 0.0001$). The linear relationship between the two variables was accomplished by Pearson correlation analysis. Pearson correlation coefficient $r < 0$ indicates negative correlation, $r > 0$ represents positive correlation, and no correlation is indicated when $r = 0$. For post hoc analysis following one-way ANOVA, the Tukey's Honestly Significant Difference (HSD) test was used to determine which specific groups differed significantly from each other when the ANOVA showed a significant result. The Tukey's HSD test controls the family-wise error rate, ensuring that the overall Type I error rate is maintained at the desired level (commonly $\alpha = 0.05$) across all multiple comparisons.

3. Result

3.1 THBS4 is Highly Expressed in the Serum of CKD Patients

Serum was collected from 100 patients diagnosed with CKD as well as from 30 healthy people. ELISA assay showed significantly higher serum levels of THBS4 in CKD patients compared to healthy control population (Fig. 1A; $p < 0.05$). The estimated glomerular filtration rate (eGFR) is an important indicator for determining CKD patients. The staging of CKD is mainly based on the patient's eGFR, the lower the eGFR, the higher the CKD stage, CKD stage 5 is the uremic stage, the patient's eGFR is extremely low. Correlation analysis was done between serum THBS4 levels and eGFR in CKD patients, and the findings revealed that serum THBS4 concentration was negatively associated with eGFR (Fig. 1B; $r = –0.77$, $p < 0.05$). This suggests that THBS4 expression is elevated as eGFR decreases, i.e., as CKD stage increases. Next, we analyzed the relationship between THBS4 concentration and patient's stage, and the results showed that THBS4 expression in the serum of CKD patients was significantly higher than that of controls, and in serum of CKD 3-5 patients was significantly higher than that of CKD 1-2 (Fig. 1C; $p < 0.05$ for both comparisons). The above results indicated that THBS4 was closely related to renal fibrosis.

3.2 THBS4 is Highly Expressed in the UUO Renal Fibrosis Model

A mouse UUO model was constructed to reveal the expression of renal fibrosis-related indexes. qPCR showed that *COL1A1*, encoding *Fibronectin* (*FN1*), as well as *encoding α-SMA* (*ACTA2*) were significantly elevated after UUO surgery compared with the sham-operated (Sham) group (Fig. 2A; $p < 0.05$ for all comparisons). WB results revealed that protein expression of COL1A1, α-SMA as well as Fibronectin was significantly increased in the UUO group compared to the Sham group (Fig. 2B,C; $p < 0.05$ for all comparisons). These results suggested that our mouse renal fibrosis model was successfully constructed. PAS and Masson staining also showed renal mesenchymal injury with fibrotic lesions. IHC findings indicated a notable elevation in THBS4 expression within the kidneys of the UUO group (Fig. 2D,E, $p < 0.05$). The qPCR results showed that the mRNA expression of *THBS4* was significantly increased in the kidney tissues of UUO mice (Fig. 2F; $p < 0.05$). These findings indicate THBS4 is significantly upregulated during the progression of renal fibrosis.

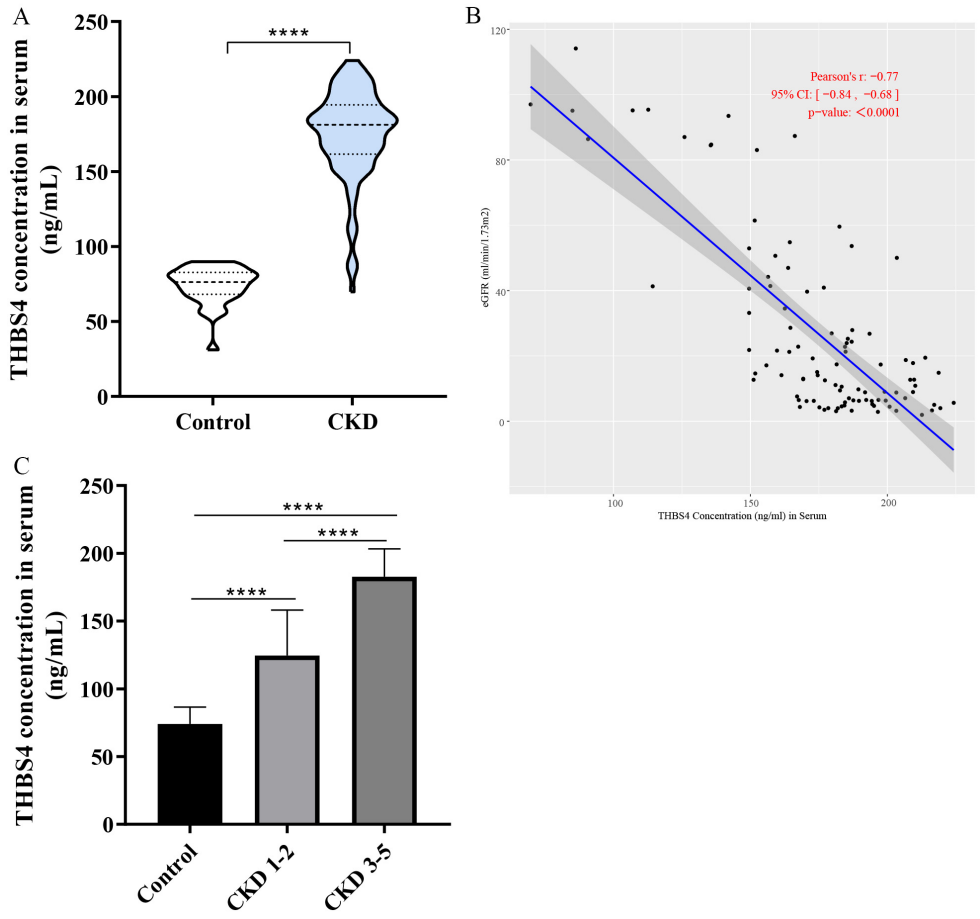

Fig. 1. Expression analysis of THBS4 in clinical CKD patients. (A) Expression analysis of THBS4 in serum of CKD patients and healthy population. (B) Correlation analysis of THBS4 content with eGFR. (C) Relationship between THBS4 content and staging of CKD patients. Control, n = 30; CKD, n = 100. ****$p < 0.0001$. THBS4, thrombospondin-4; CKD, Chronic kidney disease; eGFR, estimated glomerular filtration rate.

3.3 Reduced THBS4 Expression Inhibits TGF-β1-Induced HK2 Cell Fibrosis

To ensure the efficacy of *THBS4* knockdown, both protein and mRNA levels were assessed. qPCR analysis showed a significant decrease in *THBS4* mRNA expression in the si-*THBS4* group (Fig. 3A; $p < 0.05$). These validation experiments confirm that si-*THBS4* effectively knocks down *THBS4* expression, supporting the reliability of the observed anti-fibrotic effects. Similarly, Western Blot analysis demonstrated that THBS4 protein expression was significantly reduced in the si-*THBS4* group compared to the si-NC group (Fig. 3B,C; $p < 0.05$). TGF-β1, a potent fiber-forming factor, was used to induce HK2 cell fibrosis model. Cells were transfected with si-NC and si-*THBS4* vectors and given TGF-β1 intervention as an experimental group (si-NC+TGF-β1, si-*THBS4*+TGF-β1), and the control group (si-NC) was transfected with si-NC vector only without TGF-β1 intervention. The qPCR results revealed a notable upregulation in the expression of *COL1A1*, *FN1*, *ACTA2* and *THBS4* after TGF-β1 stimulation contrasted with the si-NC group. *COL1A1*, *FN1*, *ACTA2* and *THBS4* was suppressed in the si-*THBS4*+TGF-β1 group contrasted with the si-NC+TGF-β1 group (Fig. 3D–G; $p < 0.05$ for all comparisons). Consistent with the qPCR results, WB showed that interfering with THBS4 expression inhibited COL1A1, Fibronectin, α-SMA protein expression (Fig. 3H; $p < 0.05$ for both comparisons). This suggests that TGF-β1 stimulation induced HK2 cell fibrosis, and interfering with THBS4 expression could inhibit the process of HK2 cell fibrosis.

3.4 Knockdown of THBS4 Attenuates Renal Fibrosis in UUO Mice

Control mice (scramble) and *THBS4* knockdown mice (shRNA-*THBS4*) were purchased. To confirm the efficacy of *THBS4* knockdown *in vivo*, both mRNA and protein levels were assessed in kidney tissues from control mice and *THBS4* knockdown mice. qPCR analysis revealed a significant reduction in *THBS4* mRNA expression in knockdown mice compared to control mice (Fig. 4A; $p < 0.05$). Consistent with these findings, Western Blot analysis demonstrated that THBS4 protein expression was signifi-

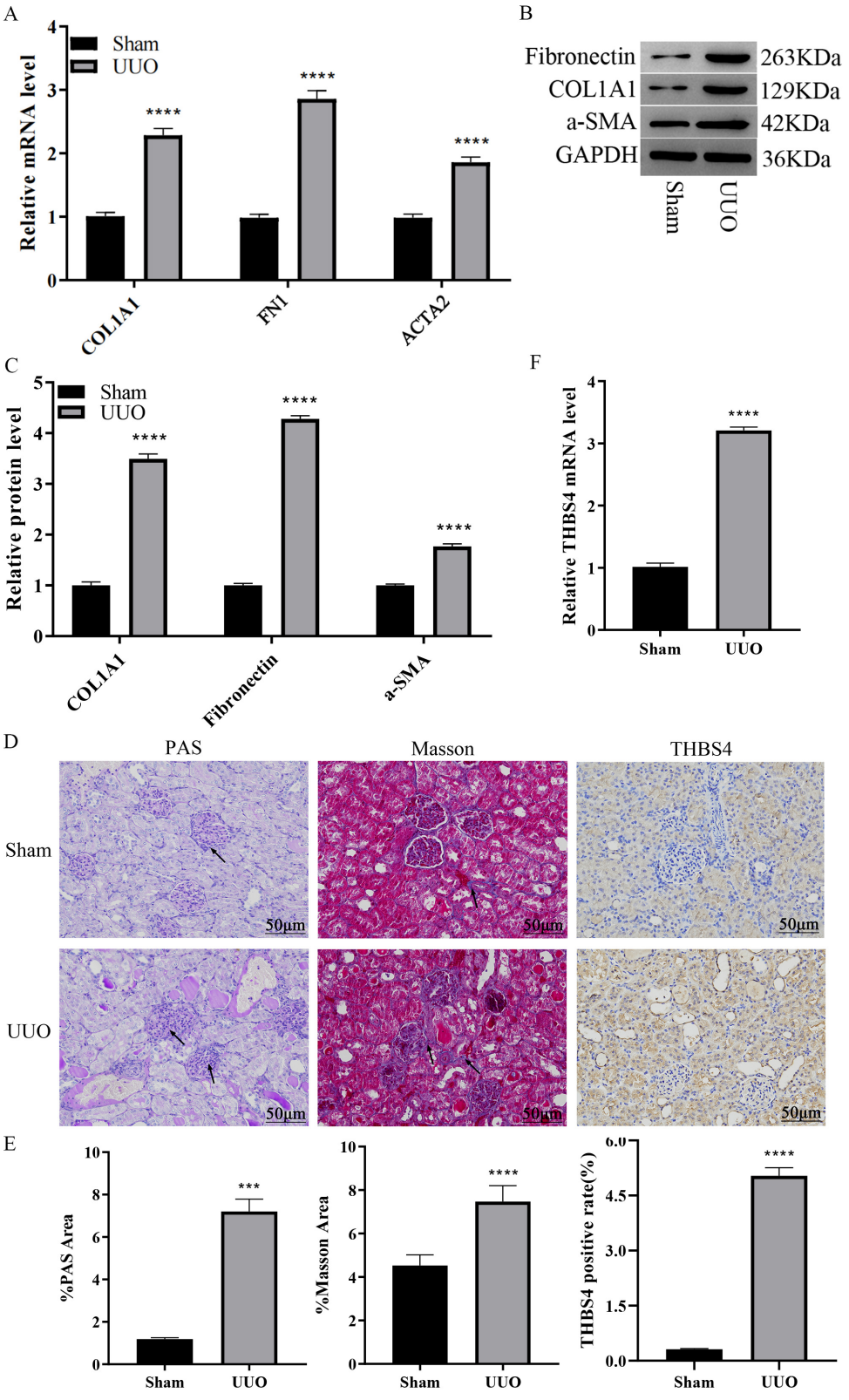

Fig. 2. Expression analysis of THBS4 in the mouse UUO model. (A) qPCR detection of mRNA expression changes of renal fibrosis indexes after UUO. (B,C) WB detection of protein expression changes of renal fibrosis indexes after UUO. (D) PAS, Masson staining, and IHC for detection of renal fibrotic lesions; Magnification factor: 200×. Scale bar = 50 μm. (E) Quantitative analysis of the figure (D). (F) *THBS4* mRNA expression in mouse kidney tissue. n = 6. There is a significant difference compared to the Sham group, with ***$p < 0.001$ and ****$p < 0.0001$. UUO, unilateral ureteral obstruction; qPCR, real-time quantitative PCR; WB, Western Blotting; PAS, Periodic Acid-Schiff Stain; IHC, immunohistochemical.

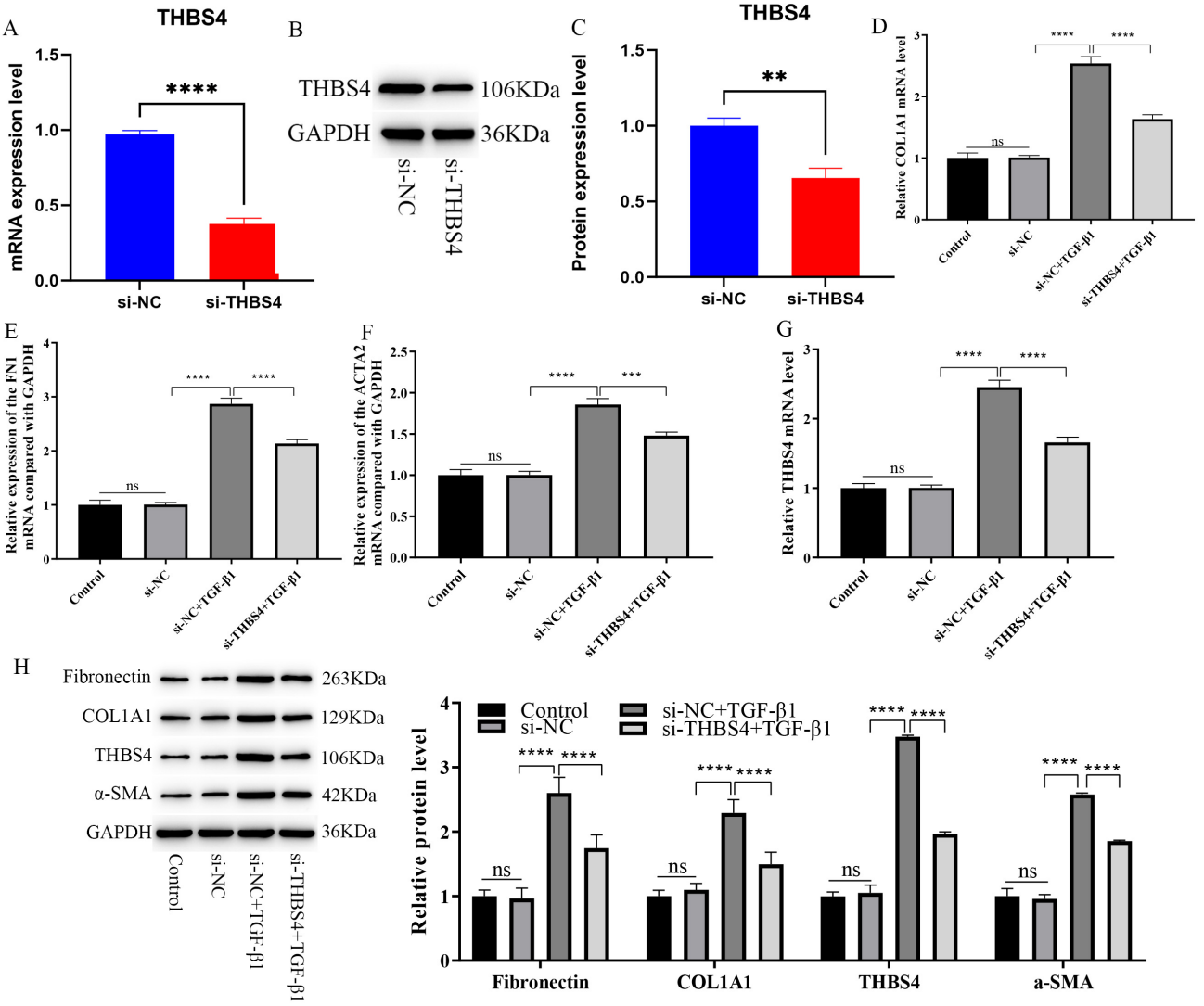

Fig. 3. Effect of inhibiting *THBS4* expression on HK2 cell fibrosis. (A) qPCR validation of *THBS4* mRNA knockdown. (B,C) WB validation of THBS4 protein knockdown. (D–G) qPCR detection of the effect of inhibiting *THBS4* expression on TGF-β1-induced renal fibrosis. (H) WB detection of the effect of inhibiting THBS4 expression on TGF-β1-induced renal fibrosis. n = 3. $^{**}p < 0.01$, $^{***}p < 0.001$, $^{****}p < 0.0001$. The ns indicates no significant difference. HK2, Human Kidney-2; TGF-β1, transforming growth factor β1.

cantly lower in knockdown mice compared to control mice (Fig. 4B,C; $p < 0.05$). All mice were taken 14 days after UUO modeling, with the contralateral kidney as a control (Sham). PSR and Masson staining was performed on kidney tissue sections, which revealed increased renal interstitial fibrosis after UUO modeling. The semi-quantitative assessment of PSR and Masson findings revealed a significant increase in the extent of renal fibrosis within the UUO group contrasted with the Sham group. Knockdown of *THBS4* followed by UUO modeling showed that the PSR and MTC-positive area were significantly lower in knockdown mice compared with control mice (Fig. 4D–G; $p < 0.05$ for both comparisons). This indicated that renal fibrosis was alleviated in mice after knocking down *THBS4*. The qPCR assay revealed a significant upregulation in the expression of *COL1A1*, *FN1*, and *ACTA2* in the kidneys of the UUO model compared to the Sham group. Whereas knockdown of *THBS4* followed by the construction of the UUO model resulted in down-regulation of the expression levels of these fibrosis indicators in kidney tissues, which was statistically different compared with control mice (Fig. 4H; $p < 0.05$ for both comparisons).

3.5 Knockdown of THBS4 Affects the Renal Fibrosis Process by Inhibiting the Activation of PI3K/AKT Pathway

The above experiments have confirmed that interfering with THBS4 expression can inhibit the renal fibrosis process. We next explored its mechanism of action. *In vitro*, WB analysis showed that the protein expression ratios of p-PI3K/PI3K and p-AKT/AKT were significantly increased in HK2 cells following TGF-β1 intervention compared with the si-NC group. After THBS4 interference

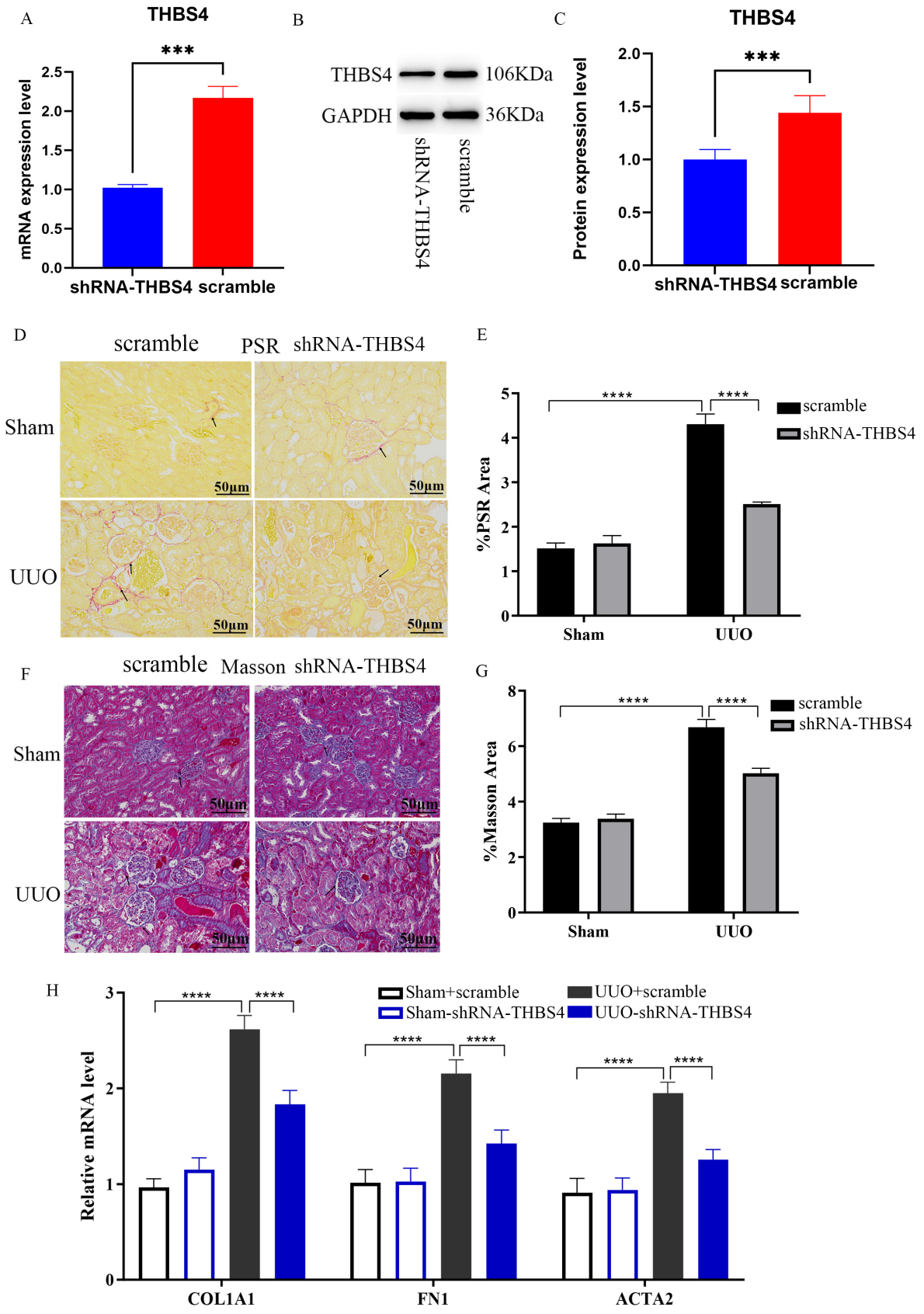

Fig. 4. Mechanism study of THBS4 regulating the process of renal fibrosis. (A) qPCR validation of *THBS4* mRNA knockdown in kidney tissues. (B,C) WB validation of THBS4 protein knockdown in kidney tissues. (D–G) PSR and Masson staining to detect the fibrosis of mouse kidney after *THBS4* knockdown. Scale bar = 50 μm. (H) qPCR to detect the effect of *THBS4* knockdown on the expression of renal fibrosis indicators in mice. n = 6. ***$p < 0.001$, ****$p < 0.0001$. PSR, Picro Sirius Red.

treatment, the levels of p-AKT/AKT and p-PI3K/PI3K exhibited a significant decrease (Fig. 5A,B; $p < 0.05$ for all comparisons), indicating that *THBS4* knockdown inhibits TGF-β1-induced activation of the PI3K/AKT pathway. To further validate this finding, additional experiments were conducted where HK2 cells were treated with TGF-β1 and transfected with si-NC or si-*THBS4*, followed by IGF-1 (100 ng/mL) or solvent. Western Blot analysis revealed that the protein expression ratios of p-PI3K/PI3K and p-AKT/AKT were significantly reduced in the si-*THBS4* + activator control group compared to the si-NC + activator control group ($p < 0.05$). Furthermore, IGF-1 treatment (si-*THBS4* + activator) partially rescued the suppression of PI3K/AKT pathway activation caused by *THBS4* knockdown, as evidenced by increased p-PI3K/PI3K and p-AKT/AKT ratios compared to the si-*THBS4* + activator control group ($p < 0.05$) (Fig. 5C,D). Meanwhile, we assessed the expression of *COL1A1*, *FN1*, *ACTA2* and *THBS4* via qPCR (**Supplementary Fig. 1**), which showed that their expression was significantly decreased in the si-*THBS4* + activator control group and partially restored by IGF-1 treatment in the si-*THBS4* + activator group. These results indicate that *THBS4* knockdown inhibits the activation of the PI3K/AKT pathway, thereby reducing renal fibrosis. *In vivo*, the UUO model group exhibited significantly elevated p-AKT/AKT and p-PI3K/PI3K ratios compared to the Sham group, confirming PI3K/AKT pathway activation after surgery. Knockdown of *THBS4* significantly decreased these ratios in UUO mice compared to control mice (Fig. 5E,F; $p < 0.05$), suggesting that THBS4 regulates renal fibrosis by suppressing PI3K/AKT pathway activation through inhibition of PI3K and AKT phosphorylation.

4. Discussion

In serum samples from clinical patients, we observed an inverse association between eGFR and the expression of THBS4. The higher the CKD stage, the higher the expression of THBS4. THBS4 expression was elevated in TGF-β1-stimulated HK2 cells *in vitro* and in the kidneys after UUO surgery *in vivo*. The proteins of renal fibrotic in TGF-β1-induced HK2 cells was reduced upon deletion of the *THBS4* gene. *THBS4* knockdown mice with UUO had reduced renal fibrosis and decreased expression of fibrotic proteins in the kidneys. TGF-β1 induction and UUO surgery activated the PI3K/AKT signaling pathway, and inhibition of THBS4 expression suppressed PI3K/AKT pathway activation as well. Importantly, IGF-1-mediated reactivation of PI3K/AKT signaling reversed the anti-fibrotic effects of *THBS4* knockdown.

The role of THBS4 in a variety of other diseases has been reported. THBS4 is overexpressed in tissues and cells of patients with hepatocellular carcinoma, where it regulates epithelial-mesenchymal processes and interacts with the integrin family to regulate the FAK/PI3K/AKT pathway, which in turn regulates hepatocarcinogenesis [19]. In cases of gastric cancer, there was a positive association observed between elevated THBS4 expression and higher pathological stage as well as unfavorable prognosis [20]. Overexpression of THBS4 suppresses programmed cell death in prostate cancer cells by activating the PI3K/AKT pathway and promotes tumor growth *in vivo* [21]. Keloid (KL) is a common skin tumor characterized by significant fibrosis and inflammatory response. THBS4 was found to be significantly overexpressed in KL [22]. It has been demonstrated that the expression of THBS4 is elevated in fibroblasts found in hypertrophic scars, which are subject to a fibrotic response dependent on TGF-β1 [23]. Enhancing THBS4 expression in fibroblasts resulted in elevated levels of TGF-β1 and α-SMA expression [24]. These studies indicate that THBS4 is involved in the regulation of fibrosis.

CKD is a chronic kidney disease, and the common pathological features are tubulointerstitial fibrosis will allow glomerulosclerosis. With the progression of renal fibrosis, patients with CKD experience a gradual decline in their kidney function and ultimately progress to end-stage renal disease [25]. TGF-β1 is widely recognized as a key controller of renal fibrosis, triggering the activation and conversion of fibroblasts into myofibroblasts, while also stimulating the production of proteins associated with fibrosis [26,27]. Our study found that the expression of COL1A1, Fibronectin, α-SMA, and THBS4 was significantly elevated after TGF-β1 stimulation of HK2 cells. Interference with THBS4 expression inhibited TGF-β1-induced secretion of fibronectin in HK2 cells. Animal models also showed that knockdown of *THBS4* alleviated the process of UUO-induced renal fibrosis. This indicates that THBS4 may play a promoting role in renal fibrosis.

A pharmacological investigation revealed that the primary molecular mechanism by which Fufang Shenhua tablet (SHT) intervenes in CKD involves suppressing the activity of PI3K/AKT [28]. Suppression of mir-214-3-p leads to a decrease in renal interstitial fibrosis through modulation of the PTEN/PI3K/AKT signaling pathway [29]. Aloe rhodopsin also attenuated renal fibrosis by inhibiting the PI3K/AKT/mTOR pathway [30]. A prior investigation demonstrated that the upregulation of *THBS1*, a different constituent within the THBS family, triggered the activation of the PI3K/AKT signaling pathway, thereby exacerbating renal fibrosis and promoting certain epithelial-mesenchymal transition processes [31]. These studies have shown that renal fibrosis can be attenuated in CKD patients by inhibiting the PI3K/AKT pathway. Our study has demonstrated that reduced THBS4 expression would can inhibit the process of renal fibrosis. Moreover, reduced THBS4 expression inhibited the TGF-β1-induced elevation in the phosphorylation levels of PI3K and AKT in HK2 cells. The expression of p-AKT and p-PI3K was reduced in *THBS4* knockdown mice compared with control mice after UUO. This suggests that THBS4 can inhibit the process of

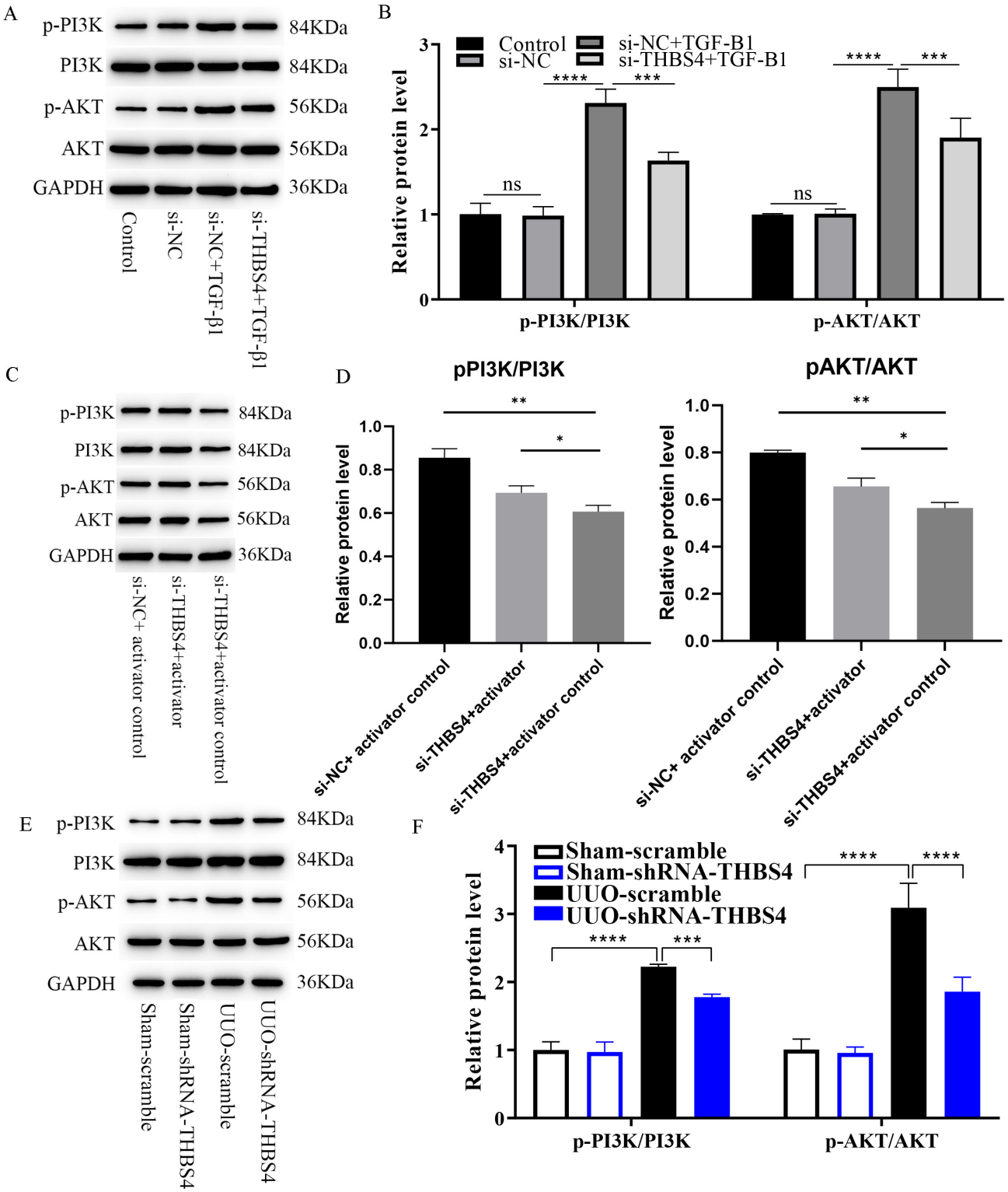

Fig. 5. Reduced THBS4 expression inhibits PI3K/AKT pathway activation. (A) WB detection of the effect of inhibition of THBS4 expression on PI3K/AKT pathway protein expression in cells, n = 3. (B) Quantitative analysis of Fig. 5A. (C) WB analysis of IGF-1 activator-treated cells with TGF-β1: THBS4 silencing suppressed PI3K/AKT pathway activation. (D) Quantitative analysis of Fig. 5C. (E) WB detection of the effect of THBS4 knockdown on PI3K/AKT pathway protein expression in mouse kidney, n = 6. (F) Quantitative analysis of Fig. 5E. *$p < 0.05$, **$p < 0.01$, ***$p < 0.001$, ****$p < 0.0001$. The ns indicates no significant difference. PI3K/AKT, phosphatidylinositol 3-kinase/protein kinase B; IGF-1, insulin-like growth factor 1.

renal fibrosis by suppressing the activation of PI3K/AKT pathway induced by TGF-β1 induction and UUO surgery.

As an important component of the extracellular matrix, THBS4 can influence the process of renal fibrosis by regulating the deposition and degradation of extracellular matrix (ECM) [32]. The results of this study suggest that THBS4 expression is up-regulated in renal fibrosis models, and inhibition of *THBS4* gene expression can reduce the degree of renal fibrosis. This suggests that THBS4 can be a potential target for early diagnosis and treatment of CKD. And unlike traditional therapies that focus on controlling risk factors for disease progression, therapies targeting THBS4 are directly aimed at the core mechanisms of renal fibrosis and thus may be more specific and effective.

5. Conclusion

Overall, based on clinical samples, cellular experiments and animal models, we found that THBS4 expression was upregulated in CKD and positively correlated with CKD patient stage and negatively correlated with eGFR. Inhibition of THBS4 can inhibit the secretion of fibrosis-related proteins and PI3K/AKT pathway activation to alleviate renal fibrosis. These results may contribute to the study of the molecular mechanisms of CKD disease. Despite this, there are still some limitations in this study, such as the sample size included in the study is not large enough, the mechanism of THBS4 regulating the PI3K/AKT pathway is not detailed enough, and there is a lack of direct role of THBS4 in the treatment of CKD. These are the focus of our further research in the future.

Availability of Data and Materials

The datasets used and analyzed during the current study are available from the corresponding author on reasonable request.

Author Contributions

XY and YZ designed the research study. XY and YY performed the research. KZ provided help and advice on the experiments. WS and LW analyzed the data. XY drafted the manuscript. All authors contributed to editorial changes in the manuscript. All authors read and approved the final manuscript. All authors have participated sufficiently in the work and agreed to be accountable for all aspects of the work.

Ethics Approval and Consent to Participate

The study was approved by the Second Affiliated Hospital of Qiqihar Medical University Ethics Committee (ethics number: [2022]0815-8-2) and patients or their families/legal guardians in the study gave informed consent. This study strictly adheres to the ethical principles and guidelines of the Declaration of Helsinki. All animal experiments comply with the international ethical standards for experimental animals and the regulations designated by the Second Affiliated Hospital of Qiqihar Medical University Ethics Committee (ethics number: [2022]0815-8-2).

Acknowledgment

Not applicable.

Funding

This work was supported by the Health Commission of Heilongjiang Province Scientific Research Topics (grant numbers 2022030350618).

Conflict of Interest

The authors declare no conflict of interest.

Supplementary Material

Supplementary material associated with this article can be found, in the online version, at https://doi.org/10.31083/FBL26076.

References

[1] Provenzano M, Coppolino G, De Nicola L, Serra R, Garofalo C, Andreucci M, *et al*. Unraveling Cardiovascular Risk in Renal Patients: A New Take on Old Tale. Frontiers in Cell and Developmental Biology. 2019; 7: 314. https://doi.org/10.3389/fcell.2019.00314.

[2] AIRG-E, EKPF, ALCER, FRIAT, REDINREN, RICORS2040, *et al*. CKD: The burden of disease invisible to research funders. Nefrologia. 2022; 42: 65–84. https://doi.org/10.1016/j.nefroe.2021.09.005.

[3] Murton M, Goff-Leggett D, Bobrowska A, Garcia Sanchez JJ, James G, Wittbrodt E, *et al*. Burden of Chronic Kidney Disease by KDIGO Categories of Glomerular Filtration Rate and Albuminuria: A Systematic Review. Advances in Therapy. 2021; 38: 180–200. https://doi.org/10.1007/s12325-020-01568-8.

[4] Adair KE, Bowden RG. Ameliorating Chronic Kidney Disease Using a Whole Food Plant-Based Diet. Nutrients. 2020; 12: 1007. https://doi.org/10.3390/nu12041007.

[5] Walker M, Godin M, Pelling AE. Mechanical stretch sustains myofibroblast phenotype and function in microtissues through latent TGF-β1 activation. Integrative biology. 2020; 12: 199-210. https://doi.org/10.1093/intbio/zyaa015.

[6] Escalona E, Olate-Briones A, Albornoz-Muñoz S, *et al*. Neu1 deficiency and fibrotic lymph node microenvironment lead to imbalance in M1/M2 macrophage polarization. Frontiers in immunology. 2024; 15: 1462853. https://doi.org/10.3389/fimmu.2024.1462853.

[7] Gu YY, Liu XS, Huang XR, Yu XQ, Lan HY. Diverse Role of TGF-β in Kidney Disease. Frontiers in Cell and Developmental Biology. 2020; 8: 123. https://doi.org/10.3389/fcell.2020.00123.

[8] Lan HY. The yin and yang role of transforming growth factor-β in kidney disease. Integrative Medicine Research and Clinical Practice. 2021; 8: 1.

[9] Waasdorp M, de Rooij DM, Florquin S, Duitman J, Spek CA. Protease-activated receptor-1 contributes to renal injury and interstitial fibrosis during chronic obstructive nephropathy. Journal of Cellular and Molecular Medicine. 2019; 23: 1268–1279. https://doi.org/10.1111/jcmm.14028.

[10] Muppala S, Xiao R, Krukovets I, Verbovetsky D, Yendamuri R, Habib N, *et al*. Thrombospondin-4 mediates TGF-β-induced an-

giogenesis. Oncogene. 2017; 36: 5189–5198. https://doi.org/10.1038/onc.2017.140.

[11] Kim MS, Choi HS, Wu M, Myung J, Kim EJ, Kim YS, *et al*. Potential Role of PDGFRβ-Associated THBS4 in Colorectal Cancer Development. Cancers. 2020; 12: 2533. https://doi.org/10.3390/cancers12092533.

[12] Shi Y, Sun L, Zhang R, Hu Y, Wu Y, Dong X, *et al*. Thrombospondin 4/integrin α2/HSF1 axis promotes proliferation and cancer stem-like traits of gallbladder cancer by enhancing reciprocal crosstalk between cancer-associated fibroblasts and tumor cells. Journal of Experimental & Clinical Cancer Research: CR. 2021; 40: 14. https://doi.org/10.1186/s13046-020-01812-7.

[13] Tuleta I, Hanna A, Humeres C, Aguilan JT, Sidoli S, Zhu F, *et al*. Fibroblast-specific TGF-β signaling mediates cardiac dysfunction, fibrosis, and hypertrophy in obese diabetic mice. Cardiovascular Research. 2024; 120: 2047–2063. https://doi.org/10.1093/cvr/cvae210.

[14] Liu X, Xu D, Liu Z, Li Y, Zhang C, Gong Y, *et al*. THBS1 facilitates colorectal liver metastasis through enhancing epithelial-mesenchymal transition. Clinical & Translational Oncology: Official Publication of the Federation of Spanish Oncology Societies and of the National Cancer Institute of Mexico. 2020; 22: 1730–1740. https://doi.org/10.1007/s12094-020-02308-8.

[15] Zeng H, Lan B, Li B, Xie H, Zhao E, Liu X, *et al*. The role and mechanism of thrombospondin-4 in pulmonary arterial hypertension associated with congenital heart disease. Respiratory Research. 2024; 25: 313. https://doi.org/10.1186/s12931-024-02932-w.

[16] Kuroda K, Yashiro M, Sera T, Yamamoto Y, Kushitani Y, Sugimoto A, *et al*. The clinicopathological significance of Thrombospondin-4 expression in the tumor microenvironment of gastric cancer. PloS One. 2019; 14: e0224727. https://doi.org/10.1371/journal.pone.0224727.

[17] Gan KJ, Südhof TC. Specific factors in blood from young but not old mice directly promote synapse formation and NMDA-receptor recruitment. Proceedings of the National Academy of Sciences of the United States of America. 2019; 116: 12524–12533. https://doi.org/10.1073/pnas.1902672116.

[18] Liu TT, Luo R, Yang Y, Cheng YC, Chang D, Dai W, *et al*. LRG1 Mitigates Renal Interstitial Fibrosis through Alleviating Capillary Rarefaction and Inhibiting Inflammatory and Pro-Fibrotic Cytokines. American Journal of Nephrology. 2021; 52: 228–238. https://doi.org/10.1159/000514167.

[19] Guo D, Zhang D, Ren M, Lu G, Zhang X, He S, *et al*. THBS4 promotes HCC progression by regulating ITGB1 via FAK/PI3K/AKT pathway. FASEB Journal: Official Publication of the Federation of American Societies for Experimental Biology. 2020; 34: 10668–10681. https://doi.org/10.1096/fj.202000043R.

[20] Chen X, Huang Y, Wang Y, Wu Q, Hong S, Huang Z. THBS4 predicts poor outcomes and promotes proliferation and metastasis in gastric cancer. Journal of Physiology and Biochemistry. 2019; 75: 117–123. https://doi.org/10.1007/s13105-019-00665-9.

[21] Hou Y, Li H, Huo W. THBS4 silencing regulates the cancer stem cell-like properties in prostate cancer via blocking the PI3K/Akt pathway. The Prostate. 2020; 80: 753–763. https://doi.org/10.1002/pros.23989.

[22] Mao J, Chen L, Qian S, Wang Y, Zhao B, Zhao Q, *et al*. Transcriptome network analysis of inflammation and fibrosis in keloids. Journal of Dermatological Science. 2024; 113: 62–73. https://doi.org/10.1016/j.jdermsci.2023.12.007.

[23] Qian W, Li N, Cao Q, Fan J. Thrombospondin-4 critically controls transforming growth factor β1 induced hypertrophic scar formation. Journal of Cellular Physiology. 2018; 234: 731–739. https://doi.org/10.1002/jcp.26877.

[24] Qian W, Zhu WH, Chen YJ, Fan JF. Role of thrombospondin-4 in fibroblasts from normal skin and hypertrophic scars. International Journal of Clinical and Experimental Medicine. 2019; 12: 1253–1260.

[25] Yuan Q, Tang B, Zhang C. Signaling pathways of chronic kidney diseases, implications for therapeutics. Signal Transduction and Targeted Therapy. 2022; 7: 182. https://doi.org/10.1038/s41392-022-01036-5.

[26] Liu BC, Tang TT, Lv LL, Lan HY. Renal tubule injury: a driving force toward chronic kidney disease. Kidney International. 2018; 93: 568–579. https://doi.org/10.1016/j.kint.2017.09.033.

[27] Chen J, Tang Y, Zhong Y, Wei B, Huang XR, Tang PMK, *et al*. P2Y12 inhibitor clopidogrel inhibits renal fibrosis by blocking macrophage-to-myofibroblast transition. Molecular Therapy: the Journal of the American Society of Gene Therapy. 2022; 30: 3017–3033. https://doi.org/10.1016/j.ymthe.2022.06.019.

[28] Li R, Shi C, Wei C, Wang C, Du H, Liu R, *et al*. Fufang Shenhua tablet inhibits renal fibrosis by inhibiting PI3K/AKT. Phytomedicine: International Journal of Phytotherapy and Phytopharmacology. 2023; 116: 154873. https://doi.org/10.1016/j.phymed.2023.154873.

[29] Hou D, Wu Q, Wang S, Pang S, Liang H, Lyu H, *et al*. Knockdown of miR-214 Alleviates Renal Interstitial Fibrosis by Targeting the Regulation of the PTEN/PI3K/AKT Signalling Pathway. Oxidative Medicine and Cellular Longevity. 2022; 2022: 7553928. https://doi.org/10.1155/2022/7553928.

[30] Huang W, Zhou P, Zou X, Liu Y, Zhou L, Zhang Y. Emodin ameliorates myocardial fibrosis in mice by inactivating the ROS/PI3K/Akt/mTOR axis. Clinical and experimental hypertension. 2024; 46: 2326022. https://doi.org/10.1080/10641963.2024.2326022.

[31] Tuoheti K, Bai X, Yang L, Wang X, Cao Y, Yisha Z, *et al*. Forsythiaside A suppresses renal fibrosis and partial epithelial-mesenchymal transition by targeting THBS1 through the PI3K/AKT signaling pathway. International Immunopharmacology. 2024; 129: 111650. https://doi.org/10.1016/j.intimp.2024.111650.

[32] Mäemets-Allas K, Klaas M, Cárdenas-León CG, Arak T, Kankuri E, Jaks V. Stimulation with THBS4 activates pathways that regulate proliferation, migration and inflammation in primary human keratinocytes. Biochemical and Biophysical Research Communications. 2023; 642: 97–106. https://doi.org/10.1016/j.bbrc.2022.12.052.